Vol. 531: 105–120, 2015
doi: 10.3354/meps11338

MARINE ECOLOGY PROGRESS SERIES
Mar Ecol Prog Ser

Published July 2

Hydroxamate siderophore secretion by *Pseudoalteromonas haloplanktis* during steady-state and transient growth under iron limitation

Ada Sijerčić, Neil M. Price*

Department of Biology, McGill University, 1205 Ave. Docteur Penfield, Montréal, Québec H3A 1B1, Canada

ABSTRACT: The kinetics of growth and siderophore secretion by *Pseudoalteromonas haloplanktis*, a γ-proteobacterium from Fe-deficient waters of the subarctic Pacific Ocean, were examined under Fe-limiting conditions. Hydroxamate siderophore concentration was about 4-fold higher in batch cultures grown in low than in high Fe medium. Addition of Fe to the Fe-limited cultures increased cell growth and electron transport system (ETS) activity and repressed siderophore secretion. In continuous culture, hydroxamate concentration increased by 4-fold and the net cellular hydroxamate siderophore secretion rate (NSSR) decreased by 20% as Fe was made more limiting to growth. An instantaneous decrease in chemostat dilution rate caused a reduction in ETS activity but had no effect on NSSR. However, pulsed addition of Fe to the chemostats significantly increased the hydroxamate concentration to a maximum within 6 to 12 h, which then subsequently declined as the cultures returned to steady state. The cellular NSSR doubled immediately after the perturbation and then dropped off to a minimum when ETS rates were fastest. Continuous addition of low levels of Fe to the chemostats increased the hydroxamate concentration in direct proportion to the quantity of Fe added, suggesting bacteria maintained tight control over Fe availability in the medium. The results show an unexpected increase in hydroxamate concentration in Fe-limited bacterial cultures following Fe enrichment and are consistent with the hypothesis that some of the Fe-binding ligands produced in iron-fertilized ocean waters are microbial siderophores.

KEY WORDS: Iron limitation · Heterotrophic bacteria · Siderophore secretion

INTRODUCTION

Siderophores are low molecular weight Fe-binding ligands produced by bacteria as part of an iron-uptake system. Siderophores scavenge and bind Fe extracellularly and are subsequently internalized as ferric siderophore complexes by specific transporters located in the bacterial outer membrane (Braun et al. 1998). Because of their strong binding constants for Fe (Witter et al. 2000) and abilities to enhance photoreductive dissolution of Fe oxides (Barbeau et al. 2001), siderophores alter chemical equilibria in ocean environments and increase the pool of Fe available for microbial growth. In pathogenic and soil bacteria, where Fe-siderophore transport systems have been well characterized, siderophore production is regulated by a ferric uptake regulator protein (Fur) that acts as a transcriptional repressor when bound to ferrous iron (Braun et al. 1998). This form of negative regulation ensures siderophores are only produced as needed, when intracellular Fe quotas fall below levels required for optimal growth.

Marine bacteria also use a siderophore-based Fe-acquisition system to survive under Fe-limiting conditions (Haygood et al. 1993, Reid et al. 1993). In a number of species, siderophore secretion is induced by low Fe concentration and repressed when adequate Fe is available (Trick 1989, Reid & Butler 1991,

*Corresponding author: neil.price@mcgill.ca

Haygood et al. 1993, Granger & Price 1999). Outer membrane receptors are induced at the same time, which bind and transport the cognate siderophore and, in some cases, heterologous siderophores (Armstrong et al. 2004). Although some heterotrophic bacteria do not secrete siderophores in Fe-limited culture, these same strains produce receptors that enable them to utilize the siderophores of unrelated species, thereby obviating the costs associated with siderophore production (Trick 1989, Granger & Price 1999).

Measurements of Fe uptake of model siderophore complexes confirm that bacteria in the ocean are equipped to utilize some types of ferric hydroxamates, including ferrioxamines B (FB) and E (Maldonado & Price 1999, Maldonado et al. 2001). Hydroxamate siderophores have been detected in surface waters of the Atlantic Ocean and sub-Antarctic (Mawji et al. 2008, Velasquez et al. 2011) and make up part of the Fe-binding ligands that complex >99.9% of dissolved Fe in the sea (Gledhill & van den Berg 1994, Rue & Bruland 1995). The exact mechanism of utilization by plankton is not yet certain and may involve Fe-siderophore transport or ferric chelate reductases that make the complexed Fe available through a reductive step (Braun et al. 1998). Biosynthetic genes for siderophores and components of putative siderophore transporters have been identified in marine bacterial genomes and metagenomic databases from the North Atlantic and Pacific Oceans, so the metabolic machinery for Fe-siderophore uptake systems exists in some members of the prokaryotic community (Hopkinson & Barbeau 2012).

New Fe is supplied intermittently to the surface ocean by atmospheric deposition (Duce & Tindale 1991) and upwelling (Archer & Johnson 2000). How such Fe inputs affect microbial processes and siderophore production is largely unknown, although their effects on autotrophic production are well documented (Young et al. 1991, Bishop et al. 2002). In ecosystem-scale Fe-enrichment experiments, changes in Fe chemistry (Rue & Bruland 1997, Croot et al. 2001, Boye et al. 2005, Wong et al. 2006, Kondo et al. 2008) and growth of bacteria have been closely monitored (Cochlan 2001, Hall & Safi 2001, Arrieta et al. 2004, Hale et al. 2006, Kudo et al. 2009, Adly et al. 2015). These studies showed an increase in the concentration of unidentified Fe-binding ligands (FeBL) that complex all of the added Fe soon after Fe injection and an increase in bacterial production. Coincident with the increase in FeBL during the subarctic ecosystem response to iron-enrichment study (SERIES), Adly et al. (2015) observed upregulation of an ^{55}Fe-FB binding protein in bacteria and a 2- to 4-fold increase in uptake rate of the Fe siderophore complex Fe-FB, suggesting that bacterial siderophore uptake systems were enhanced by Fe addition and that some portion of the FeBL produced were likely siderophores. What is less clear is why siderophores would be produced after Fe injection since siderophore production is typically repressed under high-Fe conditions.

Only a few laboratory studies have investigated the effect of Fe enrichment on siderophore production by bacteria. These show a decrease in siderophore concentration when increasing amounts of Fe are added to Fe-limited chemostat cultures (Fekete et al. 1983) or when the degree of Fe limitation is reduced by increasing the chemostat dilution rate (Jacques et al. 2003, Folsom et al. 2014). No research thus far has examined the effects of transient Fe additions on siderophore production in marine bacteria.

MATERIALS AND METHODS

Study organism

Pseudoalteromonas haloplanktis, strain Neptune, a Gram-negative heterotrophic γ-proteobacterium from Fe-deficient waters of the NE subarctic Pacific Ocean (Armstrong et al. 2004), was grown in batch and continuous culture. The stock culture was stored in liquid N_2 in artificial seawater with 20% DMSO and re-cultured as required on seawater-based agar plates supplemented with 0.4 g bactopeptone l^{-1}. Experimental cultures were initiated from single colonies.

Batch cultures

Bacteria were grown at 20°C in the artificial seawater medium Aquil, prepared and sterilized according to the procedure of Price et al. (1989). The medium was buffered at pH 8.2 with 0.5 µmol Tris l^{-1} (Tris: 2-amino-2-hydroxymethyl-propane-1,3-diol) and supplemented with 340 µmol NH_4^+ l^{-1}, 100 µmol PO_4^{3-} l^{-1}, 2 g bactopeptone l^{-1} (Difco) and 2 g casein hydrolysate l^{-1} and vitamins. All nutrients, organic compounds, and Tris buffer were purified of trace metals with Chelex 100 (Bio-Rad) and added as filter-sterilized solutions (0.2 µm filter; Acrodisc). Trace metals were added to the medium according to Granger & Price (1999). No Fe was added to the Fe-deplete medium, and 2 µmol Fe l^{-1} was added to Fe-replete media as $FeCl_3$ (made in 0.01 mol HCl l^{-1}).

Ethylenediaminetetraacetic acid (EDTA) was purposefully omitted from the recipe. Bacteria were acclimated to Fe-deplete and Fe-replete media for at least 8 generations and used to inoculate 1 l polycarbonate flasks. Culture flasks were continuously aerated with laboratory air that was sequentially bubbled through 10% HCl and 18.2 MΩ Milli-Q water (Millipore) and then filtered through a 0.2 µm filter (Acrodisc). All culturing procedures were performed using sterile, trace-metal clean techniques.

Chemostat cultures

A chemostat was constructed from a 250 ml polycarbonate flask with input, output, air and sampling ports passing through the cap. Medium was supplied by an adjustable, continuous-flow, ceramic-piston pump (Fluid Metering Incorporation), and mixing was provided by continuous aeration as described above. The medium reservoir, pump and chemostat were thoroughly cleaned with soapy water (Micro-90®) and then sequentially soaked in reverse osmosis-treated water, 10% HCl and Milli-Q water. The entire assembly was sterilized by autoclaving.

The composition of the chemostat medium was identical to that used for the Fe-deplete batch cultures, except in the press perturbation experiments which contained ¼ of the concentration of the organic enrichment. The volume of the chemostat was maintained at 110 ml, and flow rates were adjusted to give a range of dilution rates. Steady state was achieved once bacterial biomass varied by <5% between successive samples taken at 4 h intervals (corresponding roughly to 1 to 2 generations). All chemostats were maintained for 10 cell generations at steady state before sampling or initiating experimental procedures. Bioassays were used to verify that bacteria were Fe-limited. Triplicate subsamples (10 ml) were withdrawn from the chemostat during steady state and enriched with 2 µmol Fe l^{-1} or 2 g bactopeptone l^{-1} or were left unamended (controls). Cell densities of the samples were measured after 24 h.

Bacterial abundance and growth rate

Bacterial biomass was measured by absorbance at 600 nm (A_{600}) with a Cary 1E UV-VIS spectrophotometer (Varian). Samples were diluted as necessary to keep $A_{600} \leq 1$ and within the linear range of Beer's Law. Cell density was determined by direct counting using 4′,6-diamidino-2-phenylindole (DAPI) as described by Velji & Albright (1986). The relationship between absorbance and cell density was linear: cell density (cells l^{-1}) = $7.25 \times 10^{11} \times (A_{600}) + 8.86 \times 10^{10}$, $r^2 = 0.849$; n = 13; $p < 0.0001$. Growth rates were calculated from the slope of the natural log-linear regression of A_{600} over time during the exponential phase of growth. Photographs of DAPI-stained bacteria were taken with a Nikon Eclipse 80*i* microscope equipped with a QICAM FAST 1394 camera. Surface area and volume of cells were determined using the Simple PCI program (Compix).

Hydroxamate siderophore measurements

Hydroxamate concentration was determined by a modified Csaky assay using hydroxylamine as a standard (Gillam et al. 1981). Samples were withdrawn from the cultures by sterile syringe and gently filtered through a 0.75 µm glass fiber filter (AMD Manufacturing) and then a 0.2 µm filter (Acrodisc; acrylic membrane) prior to analysis. The detection limit for the assay, defined as 3 times the standard deviation of the blank sample, was 1.2 µmol hydroxylamine equivalents l^{-1}.

Electron transport system (ETS) activity

Bacteria were harvested by centrifugation in 50 or 250 ml tubes at 10 000 × *g* for 40 min at 4°C. The pellet was re-suspended in 1.6 ml of grinding buffer (0.05 mol phosphate buffer l^{-1}, pH 8.0, 0.15% polyvinylpyrrolidone, 2 mmol KCN l^{-1}, 0.15 mmol $MgSO_4$ l^{-1} and 0.1% Triton X-100) and stored frozen at −70°C for up to 2 wk. Frozen samples were thawed and sonicated using a Branson Sonifier 450 (output control = 3, duty cycle = 50%) for two 30 s bursts, cooling the sonicator tip in ice water between bursts. Cell debris was removed by centrifugation, and the supernatant was assayed immediately for ETS activity. Protein concentration was determined by the bicinchoninic acid method (Smith et al. 1985), using bovine serum albumin as a standard. Separate experiments established that no protein was lost during the preparation of cell-free homogenates.

ETS activity was determined by measuring the rate of formazan production from iodonitrotetrazolium (INT) at 490 nm using an extinction coefficient of 15.9 l mol^{-1} cm^{-1} (Packard & Williams 1981). Production rates were converted to units of mol O_2 consumed and normalized per unit protein. The final

reaction mixture (3.025 ml) contained 0.05 mol phosphate buffer l^{-1} (pH 8.0), 0.1 mol sodium succinate l^{-1}, 1 mmol NADH l^{-1}, 0.2 mmol NADPH l^{-1}, 0.7 mmol INT l^{-1} and 25 µl cell-free homogenate. Cell-free homogenate was diluted with grinding buffer so that the rate of formazan formation was linear for at least 4 min (~ 0.6 µg protein $µl^{-1}$ cell-free homogenate). ETS normalized to protein was not significantly affected by dilution (ANOVA, $p < 0.001$).

Batch culture experiment

Bacterial abundance, hydroxamate concentration and ETS activity were measured during exponential and stationary phase of growth in Fe-deplete and Fe-replete medium. Replicate cultures were run on separate days but sampled at the same time relative to culture inoculation. Fe-perturbation experiments were performed using Fe-deplete and Fe-replete batch cultures of *P. haloplanktis* grown into early stationary phase. About 600 ml of culture was harvested by centrifugation, as described above, once biomass reached $A_{600} \cong 1.3$ (~9×10^{11} cells l^{-1}), and the bacteria were re-suspended in an equivalent volume of Fe-deplete or Fe-replete media. All materials used during the centrifugation and re-suspension of the bacteria were sterile and acid-cleaned, as described above.

Continuous culture experiments

The chemostat was sampled in steady state for bacterial biomass, hydroxamate concentration and ETS activity. Three types of perturbation experiments were conducted: switch, pulse and press. The switch perturbation was initiated by decreasing the flow rate of the medium into the chemostat to increase the severity of Fe limitation. In the pulse perturbation, Fe was added directly to the chemostat while the flow of Fe-deplete medium was maintained. Thus, Fe concentration in the pulse perturbation increased instantaneously and then declined as it was taken up by the bacteria and diluted by the Fe-deplete media flowing into the chemostat. The concentration of Fe in the pulse addition was varied, and Milli-Q water was used as a control. In the press perturbation, Fe was added directly to the chemostat vessel and the medium reservoir so that its concentration was instantaneously increased and maintained at a constant level. In all cases, the chemostat was repeatedly sampled until the bacteria returned to steady state (or until the medium reservoir was exhausted).

Net siderophore secretion rate (NSSR; mols hydroxamate $cell^{-1}$ h^{-1}) in steady-state cultures was derived from the following equation:

$$NSSR = ([OCNO] \times DR)/CD \quad (1)$$

where [OCNO] is hydroxamate concentration in mols hydroxamate l^{-1}, DR is the chemostat dilution rate in h^{-1}, and CD is the cell density expressed as cells l^{-1}. In the transient experiments, the rate was determined from the following expression:

$$NSSR = (dOCNO/dt + ([OCNO] \times DR))/CD \quad (2)$$

where dOCNO/dt, the instantaneous rate of change in hydroxamate concentration, was calculated from the difference in [OCNO] between successive samples.

Statistical tests

Student *t*-test, ANOVA and linear least-squares regression were performed using the statistical software SYSTAT. All analyses were assigned statistical significance at $p < 0.05$.

RESULTS

Fe-deplete and -replete batch cultures

Cell density increased linearly with time when the bacteria entered stationary phase and hydroxamate siderophore concentration rose dramatically in the Fe-limited cultures, reaching 32.2 ± 0.14 µmol l^{-1} by the end of sampling (Fig. 1). Hydroxamate concentration was 7.3 ± 0.8 µmol l^{-1} under Fe-replete conditions and changed little during the experiment. Compared to the Fe-replete cultures, the low Fe treatments contained about 4-fold more hydroxamate per cell. ETS and final cell yields were also significantly different in the Fe-deplete compared to the Fe-replete cultures (0.29 ± 0.01 and 0.76 ± 0.01 µmol O_2 mg $protein^{-1}$ min^{-1}, respectively, *t*-test, $p < 0.0001$; $7.64 \times 10^{11} \pm 0.29 \times 10^{11}$ and $9.84 \times 10^{11} \pm 0.41 \times 10^{11}$ cells l^{-1} respectively, *t*-test, $p < 0.01$).

Fe-deplete batch cultures: Fe perturbation experiments

Replicate cultures of Fe-deplete *P. haloplanktis* were grown to early stationary phase, harvested and then re-suspended in fresh medium with and without

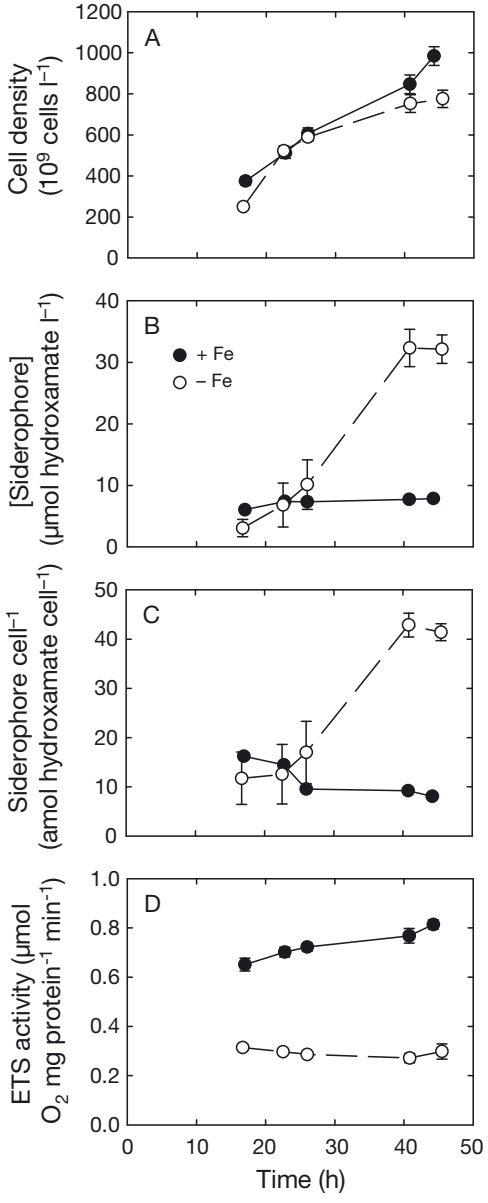

Fig. 1. Growth of batch cultures of *P. haloplanktis* in Fe-deplete (○) and Fe-replete (●) medium. (A) Cell density, (B) hydroxamate siderophore concentration, (C) hydroxamate concentration per cell and (D) electron transport system (ETS) activity. Values plotted are the mean ± standard error (SE) of 3 independent replicates

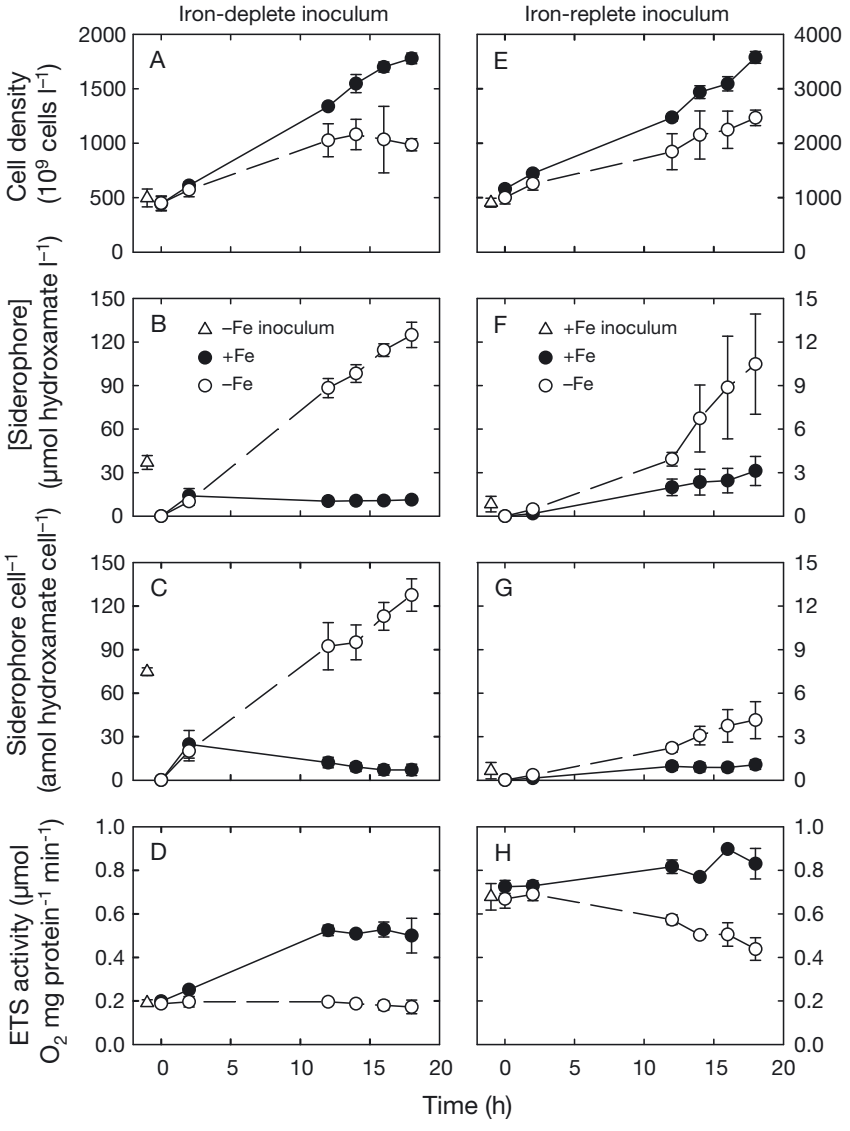

Fig. 2. Response of early stationary phase batch cultures of *P. haloplanktis* to iron perturbation. Left-hand panels show growth of iron-deplete bacteria (Fe-deplete inoculum) and right-hand panels growth of iron-replete bacteria (Fe-replete inoculum) re-suspended in fresh, iron-deplete (–Fe, ○) and iron-replete (+Fe, ●) media at Time Zero. (A,E) Cell density, (B,F) hydroxamate siderophore concentration, (C,G) hydroxamate concentration per cell and (D,H) electron transport system (ETS) activity. Initial values (△) represent the mean of 3 independent replicates obtained from the cultures used to inoculate the iron-deplete and iron-replete media. Subsequent values are the mean ± SE of 3 to 6 independent replicates

Fe (Fig. 2). ETS measurements confirmed that the bacteria were initially Fe-limited (0.19 µmol O_2 mg $protein^{-1}$ min^{-1}) and in the presence of high Fe recovered quickly and became Fe-replete. Within as little as 2 h, ETS rates were significantly faster in the Fe-replete than in the no-Fe treatments (*t*-test, $p = 0.043$). The faster ETS rates were accompanied by faster growth rate in the high Fe treatments (*t*-test, $p = 0.016$). No change was observed in ETS activity in bacteria sub-cultured in Fe-deficient medium.

Hydroxamate siderophore concentration increased continuously in the Fe-deplete cultures until the final

sampling point. Surprisingly, hydroxamates also increased when the Fe-deplete cells were inoculated into high-Fe medium, rising from 0 to 14 µmol l^{-1} within 2 h, but then changed little thereafter (*t*-test, $p > 0.05$). Compared to the Fe-replete treatments, bacterial abundance in the Fe-deplete cultures was substantially reduced (1.78×10^{12} compared to 1.08×10^{12} cells l^{-1}, respectively).

Fe-replete batch cultures: Fe perturbation experiments

Addition of Fe-replete *P. haloplanktis* to Fe-deplete medium reduced cell growth rate, final density and ETS activity as the cells became increasingly Fe-limited. Hydroxamate siderophore concentration increased in the low-Fe cultures to ~10 µmol l^{-1} by the end of the experiment (Fig. 2). In the Fe-replete medium, bacterial ETS was the highest observed during the study, ranging from 0.72 to 0.90 µmol O_2 mg $protein^{-1}$ min^{-1}. Hydroxamate concentration also increased in the Fe-enriched cultures to about 3 µmol l^{-1}.

Fe-limited continuous cultures: steady-state measurements

Dilution rate of the chemostat cultures varied from 2.8 to 9.8 d^{-1} (Fig. 3), so at steady-state, *P. haloplanktis* was growing at about 0.2 to 0.75 of its maximum rate (12.9 ± 0.95 d^{-1}; Granger & Price 1999). Subsamples from the chemostats amended with Fe grew significantly faster than unamended controls, confirming that Fe was the growth-limiting resource (ANOVA, $p < 0.0001$) (Table 1). Replicate treatments supplied with organic C in the form of bactopeptone also had greater yields than the controls in 3 of 4 cases, possibly because C was a co-limiting resource (Tortell et al. 1996) or because the bactopeptone contained low levels of Fe despite purification. The relationship between cell density and dilution rate was well described by a logistic function ($r^2 = 0.8622$, $p < 0.01$) with the greatest change in abundance at about 8 d^{-1}. Microscopic analysis showed no significant differences in cell size in cultures maintained at 4.8, 7.2 and 8.2 d^{-1} (ANOVA, $p > 0.14$, data not shown). At steady state, hydroxamate concentration ranged from 4.7 to 19.9 µmol l^{-1} and was negatively correlated with dilution rate (ANOVA, $p < 0.0001$). Siderophore secretion rate (amol hydroxamate $cell^{-1}$ h^{-1}) and ETS activity were both positively correlated with Fe-limited growth rate (ANOVA, $p = 0.018$, $p = 0.0027$, respectively). Note that the siderophore secretion rate is a net rate (NSSR) since we only measured the change in hydroxamate concentration in the chemostats and not the influx or efflux rates of hydroxamate from the bacteria.

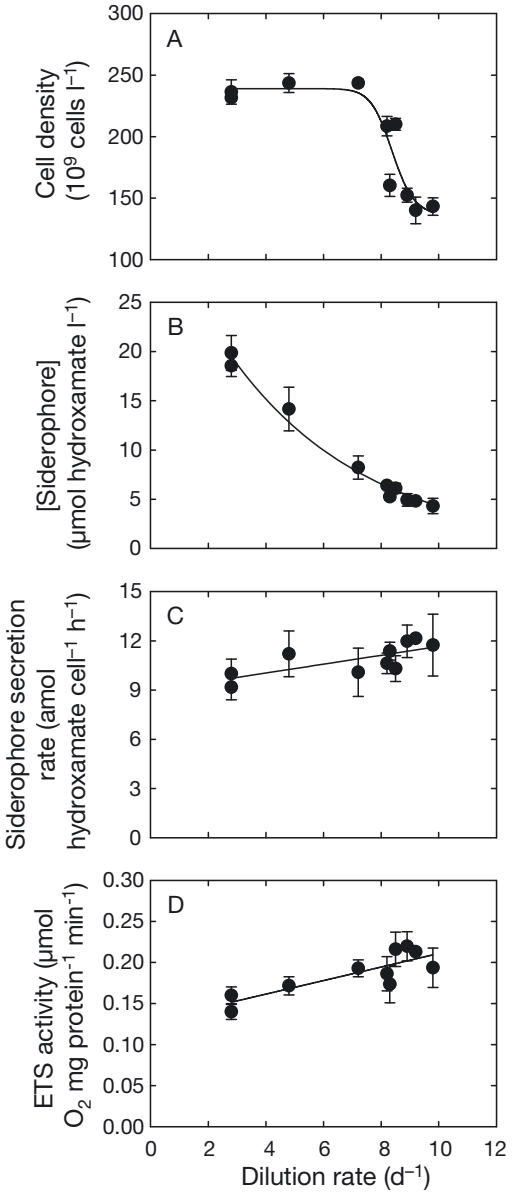

Fig. 3. Steady-state properties of Fe-limited chemostat cultures of *P. haloplanktis* as a function of dilution rate: (A) cell density, (B) hydroxamate siderophore concentration, (C) siderophore secretion rate and (D) electron transport system (ETS) activity. Values plotted are the mean ± 1 standard deviation (SD) of 3 to 7 measurements of each chemostat. Lines drawn through the data points are logistic (A), exponential (B) or linear (C,D) regressions fitted by a least squares procedure ($p < 0.05$)

Table 1. Resource limitation of chemostat cultures of *P. haloplanktis* as a function of dilution rate. Values are the mean ± standard error of cell density of 3 samples of each chemostat enriched with Fe (+Fe: 2 µmol Fe l^{-1}), C (+C: 2 g bactopeptone l^{-1}) or no addition (Control). Samples for each bioassay were obtained once the bacteria reached steady state. Different superscripts indicate significant differences among the treatments at each dilution rate (ANOVA, $p < 0.05$)

Dilution rate (d^{-1})	Cell density ($\times 10^{11}$ cells l^{-1}) Control	+ Fe	+ C
2.8	4.52 ± 0.25^a	13.0 ± 0.29^b	5.30 ± 0.25^a
4.8	5.18 ± 0.04^a	13.1 ± 0.04^b	5.90 ± 0.04^c
7.2	5.69 ± 0.12^a	13.1 ± 0.12^b	6.36 ± 0.12^c
8.2	5.16 ± 0.03^a	8.30 ± 0.03^b	5.39 ± 0.03^c

Fe-limited continuous cultures: Fe-perturbation experiments—switch

Growth kinetics and siderophore secretion were examined after the dilution rate of a chemostat was decreased from 7.2 to 2.8 d^{-1} (Fig. 4). Cell density increased by 75% from 1.70×10^{11} to 3.05×10^{11} cells l^{-1} within 5 h of the transition and then declined below the initial maximum by 30 h. Siderophore concentration also increased by 3.5-fold to about 20 µmol l^{-1} during the transition to the new steady-state, but NSSR remained constant (Fig. 4). ETS declined slightly during the experiment, confirming that the bacteria were more Fe-limited at slower dilution rate.

Fe-limited continuous cultures: Fe-perturbation experiments—pulse

Iron concentration was transiently increased by pulse addition of 2 µmol Fe l^{-1} directly to the chemostat vessels. In these experiments, a new batch of chelexed organic enrichments was used to prepare the medium for all the chemostats except 2.8 d^{-1}. The new organic enrichment affected the biomass yield of the cultures and amount of hydroxamate siderophores produced at steady state but had no effect on the kinetics of hydroxamate secretion following Fe addition. The control chemostat sampled at the same frequency as the treatments showed little change in any of the steady-state parameters over time (Fig. 5). Likewise, unperturbed chemostats varied by ≤5% in density, hydroxamate concentration and ETS activity (data not shown).

Cell density increased rapidly following Fe perturbation and within 4 to 12 h reached its maximum only to decline subsequently as the cultures returned to steady state (Fig. 5). The Fe addition stimulated ETS rates by 2-fold, but they quickly returned to pre-injection levels by 6 to 10 h. Transient increases in hydroxamate concentrations were also apparent. Statistical analysis of the slopes of regression lines describing the temporal change in hydroxamate concentration

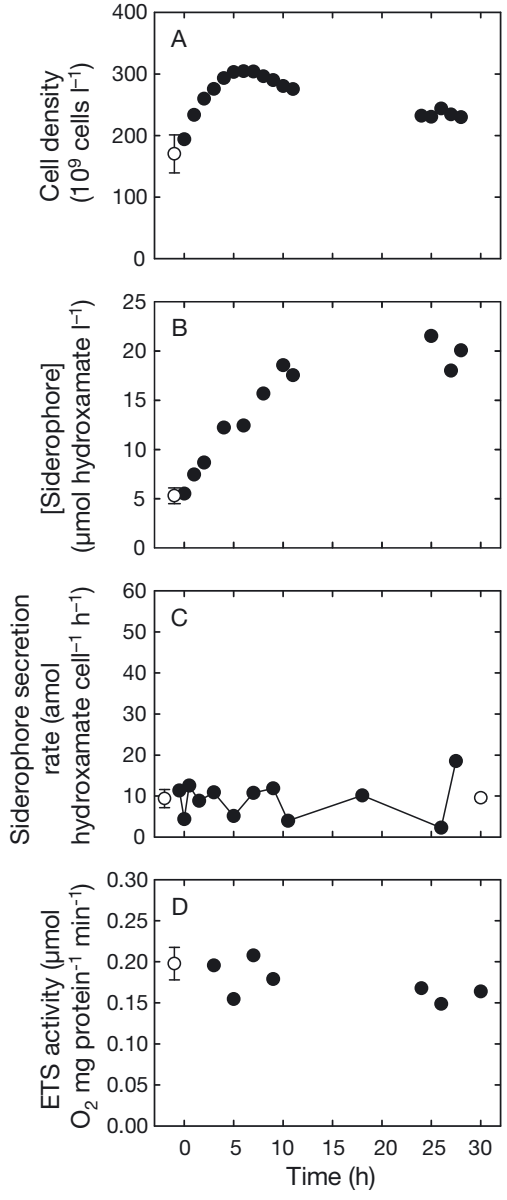

Fig. 4. Temporal change in chemostat parameters following a switch perturbation experiment: (A) cell density, (B) hydroxamate siderophore concentration, (C) siderophore secretion rate and (D) electron transport system (ETS) activity. Initial values (○) represent the mean ± 1 SD of 3 replicate chemostats of *P. haloplanktis* maintained at 7.2 d^{-1}. Subsequent measurements (●) were obtained from a single chemostat after the dilution rate was reduced to 2.8 d^{-1}, and the final value (○) was determined once cell density had reached steady state

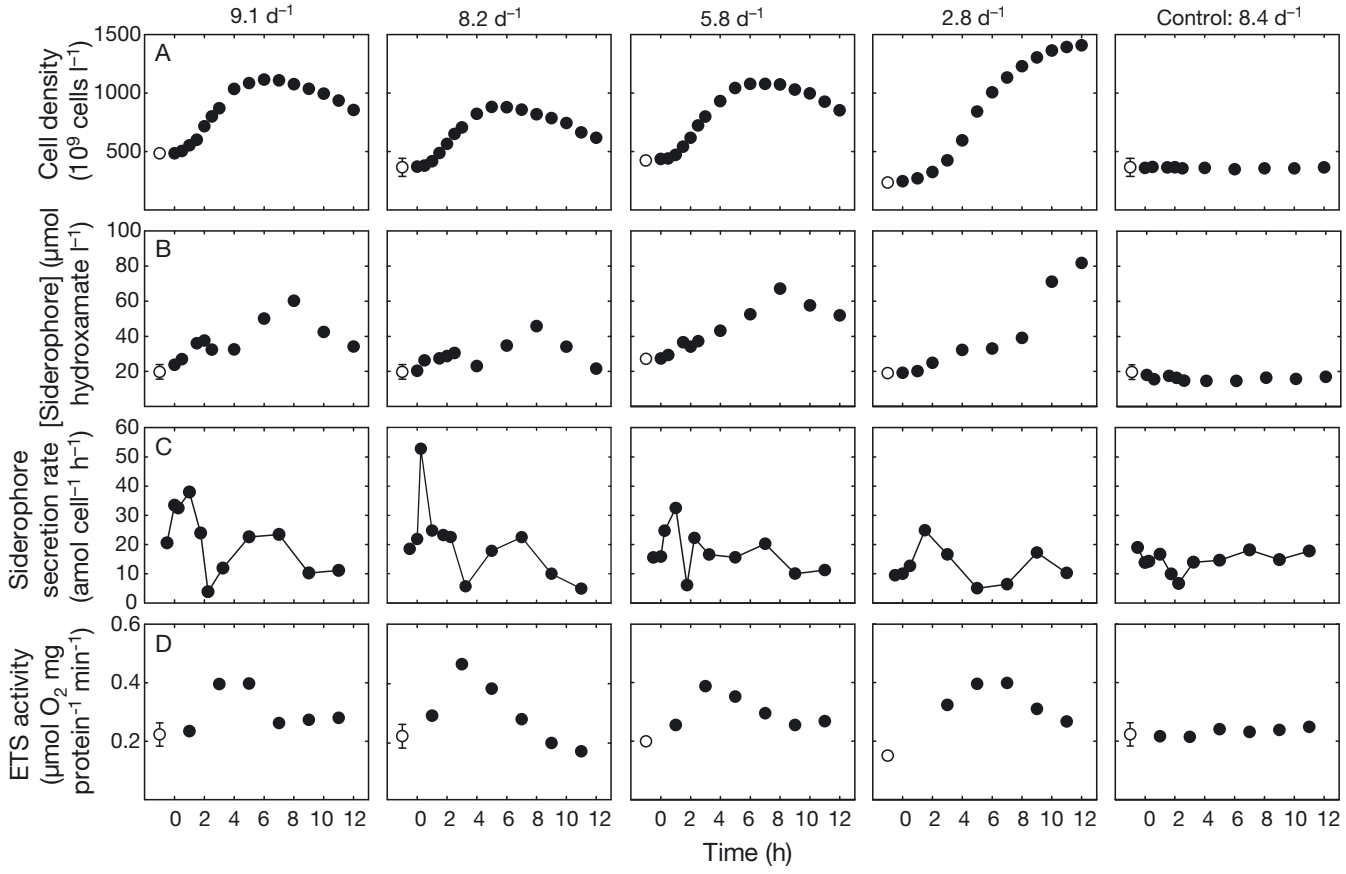

Fig. 5. Temporal change in chemostat parameters following a pulse perturbation experiment. (A) Cell density, (B) hydroxamate siderophore concentration, (C) siderophore secretion rate and (D) electron transport system (ETS) activity. Initial values (○) are the mean ± 1 SD of 3 replicate cultures of *P. haloplanktis* grown at 9.1, 8.2, 5.8, 2.8 and 8.4 d^{-1} (as indicated above). At time zero, each chemostat was enriched with 2 µmol Fe l^{-1} and sampled (●) for 12 h: the control chemostat shown on the right-hand side of the figure was enriched with an equivalent volume of Milli-Q water

over the first 8 h (chemostats: 5.8, 8.2 and 9.2 d^{-1}) or 12 h (chemostat: 2.8 d^{-1}) were significantly greater than 0 (*t*-test, $p < 0.01$), whereas no change was observed in siderophore concentration in the controls (Fig. 5). Net siderophore secretion rate peaked between 1 and 1.5 h after Fe injection and then declined. The mean rate of change in secretion rate over the first 1.5 h was 9.57 ± 3.32 amol hydroxamate cell^{-1} h^{-2} and was significantly greater than 0 ($p < 0.005$). Thus, Fe enrichment to Fe-limited *P. haloplanktis* triggered an immediate release of hydroxamate siderophore to the medium. Over the same time interval, the computed cellular secretion rate in the controls declined slightly, likely due to a small sampling artifact. The subsequent decline in secretion rate in the Fe-enriched cultures between 2 and 6 h occurred roughly when ETS activity rate was maximal. Siderophore concentration reached the highest concentration at the slowest dilution rate and only returned to steady-state about 60 h after perturbation (data not shown).

Fe-limited continuous cultures: Fe perturbation experiments — press

The transition from Fe- to C-limited growth was examined by adding 2 µmol Fe l^{-1} to a chemostat running at 8.7 d^{-1} (Fig. 6). Carbon concentration was decreased in the inflowing medium by 4-fold to ensure that it became the limiting resource after Fe was increased. Bioassay experiments confirmed that once the new steady state was established, C was the growth-limiting nutrient (ANOVA, $p = 0.00002$) (Table 2). ETS activity rapidly increased by 4- to 5-fold from the initial value of 0.108 to 0.505 µmol O_2 mg protein^{-1} min^{-1} (Fig. 6) and remained high for the duration of the experiment (~30 h, data not shown). Approximately 8 h after the Fe enrichment, cell density increased 4-fold (Fig. 6) and then remained constant. Hydroxamate concentration varied over the first 4 h, increasing by about 2 µmol l^{-1}, but then subsequently declined to undetectable levels (Fig. 6B).

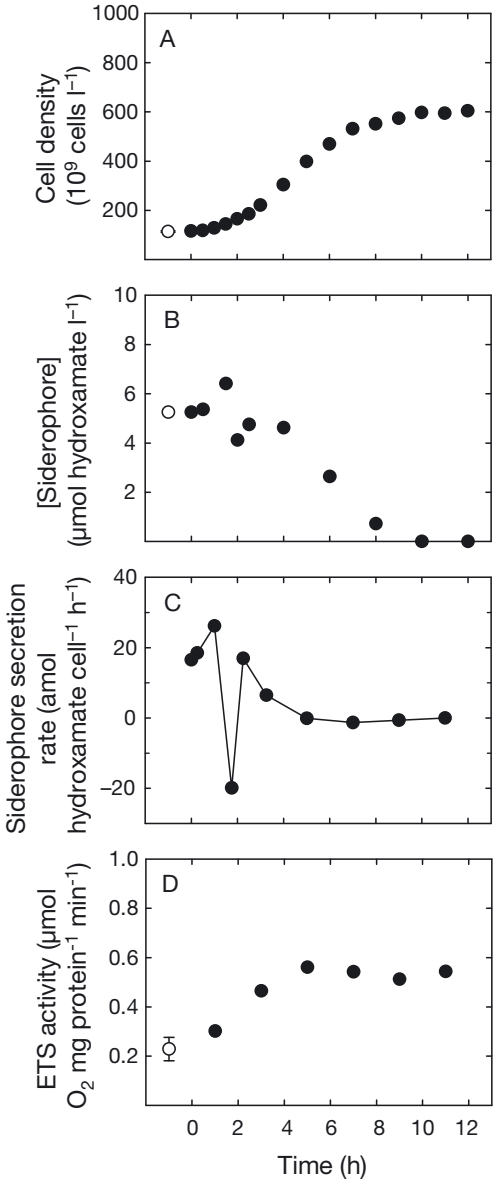

Fig. 6. Temporal change in chemostat parameters following a press perturbation experiment. (A) Cell density, (B) hydroxamate siderophore concentration, (C) siderophore secretion rate and (D) electron transport system (ETS) activity. A steady-state culture of *P. haloplanktis* grown at a dilution rate of 8.7 d^{-1} was enriched with 2 µmol Fe l^{-1} at Time Zero and repeatedly sampled (●) for 12 h. Fe was also added to the medium reservoir at the same time so that the increased Fe concentration in the chemostat was sustained throughout sampling. The medium reservoir contained ¼ of the concentration of organic C used in the pulse and switch perturbation experiments. Initial values (○) are the mean ± 1 SD of repeated measurements obtained during steady-state prior to the Fe enrichment

The rate of increase in the cellular secretion rate over the first hour (6.72 amol $cell^{-1}$ h^{-2}) was similar to that observed during the perturbation experiments reported above. Following the initial increase in secretion rate was a large decline, suggesting internalization of the siderophore. Greater variability, however, was observed at the lower hydroxamate concentrations encountered in this experiment (ca. 5 µmol l^{-1}), which may have introduced errors to these calculations.

Press experiments were also performed by adding nanomolar concentrations of iron to cultures at dilution rates of 8.2 and 8.9 d^{-1} (Fig. 7). Bioassays confirmed that these chemostats were Fe-limited even with the extra Fe addition (Table 2) and were consistent with the observed increases in cell densities at the new steady states. The increase in bacterial abundance was directly proportional to the quantity of Fe added and was accompanied by an increase in hydroxamate concentration of 0.7, 1.8 and 3.4 µmol l^{-1} in the 50, 100 and 150 nmol Fe l^{-1} enrichments, respectively (Fig. 7). Only a small increase in ETS activity was apparent after the Fe was added, and thereafter, it returned to the pre-infusion levels characteristic of Fe-limited cells. No measurements of ETS activity were made in the chemostats that received the 150 nmol Fe l^{-1} press. Cellular hydroxamate secretion rate varied little in these low-Fe treatments (Fig. 7).

The amount of additional siderophore produced (nmol d^{-1}) in the chemostat press experiments was directly proportional to the increase in the Fe supply rate (Fig. 8). Over the range of Fe concentrations tested here, approximately 23 nmol of hydroxamate was excreted per nmol of Fe added.

Table 2. Resource limitation following Fe addition to Fe-limited chemostat cultures of *P. haloplanktis*. Iron concentration [Fe press] was instantaneously increased in the chemostat and medium reservoir, and the chemostats were monitored until a new steady state was achieved. Bacterial response is reported in Figs. 6 & 7. Subsamples were subsequently removed from each chemostat at 12 h and enriched with Fe (+Fe: 2 µmol Fe l^{-1}), C (+C: 2 g bactopeptone l^{-1}) or no addition (Control). Values are the mean ± standard error of cell density of 3 replicates. The medium supplying the chemostats contained 0.5 g bactopeptone l^{-1} and 0.5 g casein hydrolysate l^{-1}, ¼ of the amount used in other experiments. Different superscripts indicate significant differences among the treatments at each dilution rate (ANOVA, $p < 0.05$)

Dilution rate (d^{-1})	[Fe press] (µmol Fe l^{-1})	Cell density (×10^{11} cells l^{-1}) Control	+ Fe	+ C
8.7	2	5.24 ± 0.07^a	5.18 ± 0.07^a	12.4 ± 0.07^b
8.2	0.15	9.37 ± 0.04^a	13.2 ± 0.04^b	10.1 ± 0.04^c
8.2	0.1	8.54 ± 0.17^a	11.91 ± 0.17^b	8.56 ± 0.17^a
8.9	0.05	6.70 ± 0.05^a	9.26 ± 0.05^b	7.39 ± 0.05^c

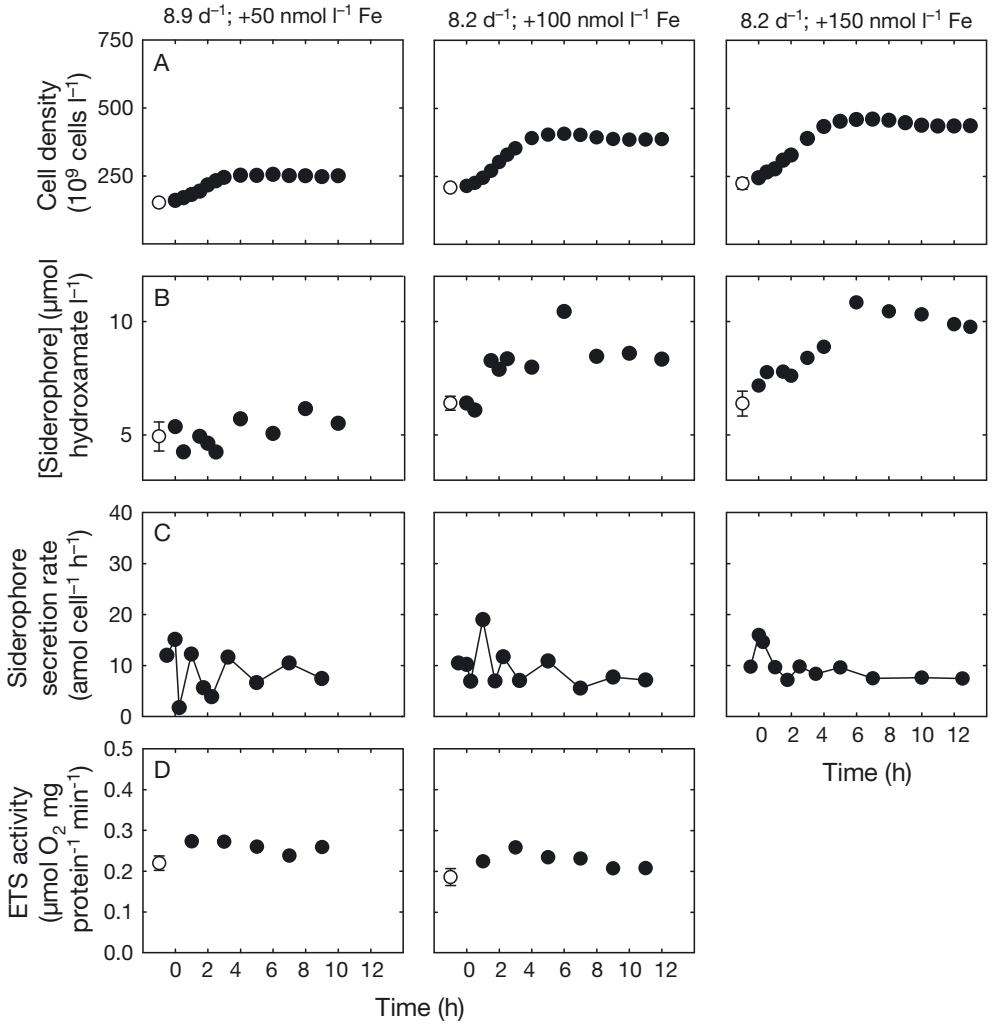

Fig. 7. Temporal change in chemostat parameters following a press perturbation experiment. (A) Cell density, (B) hydroxamate siderophore concentration, (C) siderophore secretion rate and (D) electron transport system (ETS) activity. Chemostat cultures of *P. haloplanktis* and the inflowing media were enriched with 50, 100 and 150 nmol Fe l^{-1}, as indicated above. The dilution rates of the chemostats, from left to right, were 8.9, 8.2 and 8.2 d^{-1}, respectively. Initial values (○) are the mean ± 1 SD of repeated measurements obtained during steady-state prior to the Fe press. Subsequent values (●) are single measurements

DISCUSSION

Siderophore production by γ-proteobacteria

Most of what we know about siderophore production by marine bacteria comes from laboratory studies of a few species that are easy to isolate and grow in enriched seawater medium (Vraspir & Butler 2009). These species are members of the α- and γ-proteobacteria, lineages of related species that comprise a large fraction (10 to 14%) of the bacterial types found in the sea (Acinas et al. 1999, Wietz et al. 2010). γ-proteobacteria are of particular interest and known to be most abundant in productive waters (Schattenhofer et al. 2009). Recent observations show they assimilate relatively more Fe than other bacterial groups in the Southern Ocean and the Mediterranean Sea (Fourquez et al. 2012) and that their abundance varies inversely with total dissolved Fe concentration (Royer et al. 2010). γ-proteobacteria also respond positively in Fe-enrichment bioassays in high nutrient, low chlorophyll regions (HNLC) (Hutchins 2001) and so are ecologically relevant organisms to study how Fe availability impacts microbial growth and physiology.

Previous work in our laboratory showed under Fe-limiting conditions that *P. haloplanktis*, a γ-proteobacterium from the subarctic Pacific Ocean, secretes a hydroxamate siderophore and synthesizes an outer membrane protein receptor that binds Fe(III) sidero-

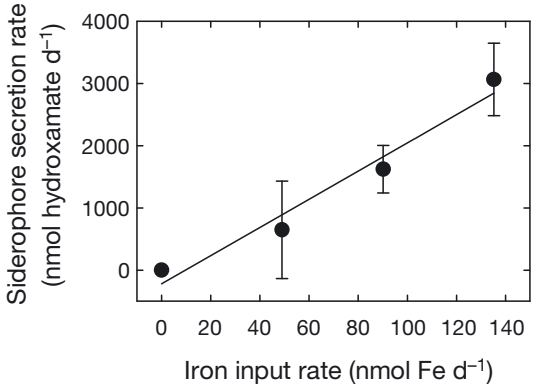

Fig. 8. Siderophore production rate in Fe-limited chemostat cultures of *P. haloplanktis* as a function of Fe input rate. Siderophore production rate corresponds to the net increase in steady-state hydroxamate concentration after the Fe press addition. The net increase in hydroxamate concentration was calculated from the difference between the initial and average of the final 3 measurements of hydroxamate concentration in the chemostats reported in Fig. 7. The Fe input rate equals the product of the flow rate and the concentration of Fe added to the chemostat. Values reported are the mean ± 1 SD. The line drawn through the data points is a linear regression fitted by a least squares procedure: $y = 22.9x - 221.0$, $r^2 = 0.9633$, $p = 0.0185$

phore complexes (Granger & Price 1999, Armstrong et al. 2004). The bacterium takes up Fe(III) bound to autologous and heterologous siderophores and is able to use it for growth (Granger & Price 1999). Rates of Fe-siderophore uptake in this species are greatly enhanced by Fe deficiency.

Experimental design

Batch and continuous cultures were used to create a range of Fe-induced physiological states and growth conditions that bacteria might naturally experience in the sea to assess how siderophore secretion changed in response to variation in Fe availability. The medium was designed to maximize siderophore production and so contained high levels of organic enrichments. EDTA was purposefully omitted from the recipe to avoid confounding effects of having another strong metal-binding ligand, in addition to the siderophore, in the medium. As a consequence of the medium design, bacterial biomass was greatly elevated compared to ocean levels, but this allowed us to use existing chemical methods to measure hydroxamate siderophore concentrations without preconcentration.

Rates of ETS activity were used to gauge the Fe nutritional status of the bacterial cells during steady-state and transient conditions. This metric was previously shown to be a good indicator of Fe limitation in aerobic heterotrophs because of its rate dependence on Fe cofactors (Tortell et al. 1996, 1999). The results reported here further illustrate this relationship: They show ETS rates varied between 0.65 and 0.9 µmol O_2 mg protein^{-1} min^{-1} in Fe-replete and between 0.15 and 0.3 µmol O_2 mg protein^{-1} min^{-1} in Fe-deplete cultures (Figs. 1 & 2), and the ETS rates were linearly related to steady-state growth rate in the Fe-limited chemostats (Fig. 3). Thus, ETS provided a sensitive and instantaneous measure of cellular Fe status that correlated with growth and could be used to assess the level of bacterial Fe during short-term experiments.

Batch cultures: perturbation results

P. haloplanktis exhibited the typical physiological response to Fe-deficient conditions by upregulating siderophore production. Other studies have also documented overproduction of siderophores by bacteria in late growth phase cultures (McIntosh & Earhart 1977, Heinrichs et al. 1999, Temirov et al. 2003) and have shown that it coincided with a significant decrease in bacterial Fe quota (McIntosh & Earhart 1977, Archibald & Devoe 1978). The observation that ETS activity remained constant while hydroxamate concentration increased suggests that large changes in Fe quota were not likely occurring during onset of siderophore secretion in *P. haloplanktis*. The ETS contains most of the cellular Fe in heterotrophic bacteria and would be expected to track Fe quota closely (Tortell et al. 1999). Siderophore production in this species appeared to be related to the slowdown in growth that occurred after 26 h (Fig. 1).

In high-Fe medium, *P. haloplanktis* was Fe-sufficient and still produced low levels of siderophore (8 µmol hydroxamate l^{-1}) (Fig. 1). Whether this represented constitutive production or was a consequence of carryover from the inoculating culture is not clear. We note that the high-Fe cultures used to inoculate the batch cultures (Fig. 1) were in stationary phase and thus may have already been mildly Fe-limited and producing siderophores. Indeed, when Fe-replete cultures were kept in exponential phase by repeated sub-culturing, they contained about ⅒ of the amount of hydroxamate reported in Fig. 1 (data not shown), suggesting that Fe may have become limiting during the later stages in the high Fe medium. Siderophore secretion has been reported in other bacteria in medium enriched with

as much as 50 µmol Fe l^{-1} so our results are not without precedent (Heinrichs et al. 1999, Temirov et al. 2003).

Fe-deplete cells continued to produce siderophores in Fe-replete medium even though ETS activity had significantly increased within 2 h (Fig. 2). Possibly, the bacteria had not yet reached an Fe-replete state and so siderophore secretion remained up-regulated. Interestingly, the initial mean rate of siderophore secretion over the first 2 h was actually faster in the presence (13.5 amol hydroxamate $cell^{-1}$ h^{-1}) than in the absence (9.7 amol hydroxamate $cell^{-1}$ h^{-1}) of added Fe, although the rates were not significantly different ($p > 0.05$). We note that siderophore concentration decreased in the Fe-enriched cultures by ca. 3.8 µmol hydroxamate l^{-1} (Fig. 2B), suggesting that some of the siderophore was reassimilated.

Chemostat: steady-state results

We anticipated that greater Fe limitation in the chemostats would enhance NSSR in part because of the large differences observed in secretion rates between the low- and high-Fe batch cultures. The batch culture results (Fig. 2) showed the rate of hydroxamate secretion was roughly 100-fold faster for the Fe-limited than for the Fe-replete bacteria (7.5 ± 2.4 versus 0.072 ± 0.032 amol hydroxamate $cell^{-1}$ h^{-1}, respectively), whereas NSSR changed little in the chemostats (Fig. 3). One likely explanation for the chemostat result is that the rate of siderophore secretion was already maximized under the Fe-restricted conditions. Indeed, transition to a more Fe-limited state had no effect on NSSR (Fig. 4). We cannot, however, rule out the possibility that siderophore secretion may have been reduced at slow growth rates because of decreased C availability. Iron limitation is known to alter gross growth efficiency (Tortell et al. 1996), which could affect the amount of C available for siderophore production. The slight but significant decline in NSSR (Fig. 3) could also reflect the large energetic costs of siderophore production (as discussed below), which could not be sustained at slow dilution rates. Bacterial density increased by about 70% as dilution rate declined, whereas the siderophore concentration increased by a factor of 4.

Chemostat: perturbation results

The temporal change in hydroxamate concentration following pulsed Fe enrichment showed biphasic kinetics and was caused by an increase in NSSR and a subsequent increase in bacterial abundance during the transient phase (Fig. 5). The initial phase was characterized by significant shift-up in NSSR ($p < 0.05$). Maximum rates of hydroxamate secretion ranged from 24 to 52 amol $cell^{-1}$ h^{-1} during this time and were 2.4-fold faster on average than the pre-enrichment values (Fig. 5). The increase in secretion rate was short-lived, as the rate subsequently declined below the initial values. The decline in NSSR could represent a slowdown in siderophore release and/or an increase in uptake as some of the Fe siderophore complex was internalized. Although our measurements cannot distinguish between these possibilities, the decrease in siderophore concentration observed in batch cultures (discussed above, Fig. 2B) suggests that the decrease in NSSR could indeed be due to siderophore uptake. ETS measurements are consistent with this interpretation. They show that bacterial physiological state increased during the initial phase of siderophore secretion, presumably as the cells internalized some of the ferrated siderophores and built up Fe stores. This Fe was then assimilated to replenish the respiratory ETS, which peaked around the time that NSSR was at a minimum. Thus, relief of Fe limitation, albeit brief, caused an apparent decrease in NSSR. The second phase of siderophore production appeared to result from an increase in bacterial biomass as growth rate of the Fe-enriched bacteria increased and NSSR returned to preinfusion levels. The eventual decline in siderophore concentration occurred once the cells and siderophore began to wash out of the chemostat. Thus, the results of these experiments show an immediate release of hydroxamate siderophore in response to Fe supply to Fe-limited cells.

Costs of siderophore secretion

The C requirements for siderophore production under Fe-limiting conditions can be estimated from the data reported in Fig. 3 by expressing the steady state production of cells and siderophore in terms of C. To make the calculation, we need to know the amount of C per cell and C per hydroxamate siderophore. Two estimates of cellular C derived from measurement of cellular protein (Simon & Azam 1989) and cell volume (Bratbak & Dundas 1984) were in good agreement: 20 and 10 fmol C $bacterium^{-1}$, respectively. The C content of the hydroxamate siderophore of *P. haloplanktis* was estimated by assuming its chemical composition was similar to

other well-characterized siderophores of marine and terrestrial bacteria. On average, hydroxamate and mixed-ligand siderophores contain about 10 mol C mol^{-1} hydroxamate or as much as 22 mol C mol^{-1} hydroxamate in the case of some amphiphilic siderophores, like marinobactin and aquachelin (Martinez et al. 2003). We used these conversion factors to calculate the minimum and maximum siderophore secretion as a percentage of net C production. As illustrated in Fig. 9, the proportion of cell C released as siderophore increased exponentially with decreasing dilution rate ($p < 0.0001$) and varied between 4 and 19% under the most Fe-limiting conditions. This represents a remarkably large quantity of C, but agrees well with our results from the batch cultures that show about 12% of the total biomass produced could be released as siderophore C (Fig. 2). Similar calculations for the pulsed Fe-addition experiments show that siderophore secretion represents an even greater fraction of the cellular C production rate during the transient phase (Fig. 9). Not considered in these calculations are the additional costs of siderophore production in terms of N, which are roughly similar to C (since the siderophore C:N ratio is ~3 to 4), nor the energy costs of active transport of siderophore back into the cell, which are assumed to be large (Mietzner et al. 1998, Volker & Wolf-Gladrow 1999). Thus, a substantial amount of C may be required to produce siderophores, which would reduce energy reserves that might otherwise be diverted to growth (Adly et al. 2015). If siderophore production is common among marine bacteria, then it could contribute to low growth efficiency in low-Fe regions of the sea.

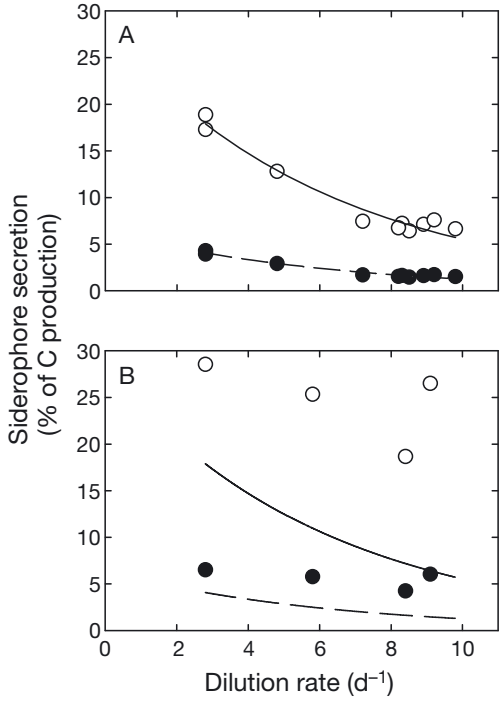

Fig. 9. Costs of hydroxamate siderophore secretion by *P. haloplanktis* as a function of Fe-limited growth rate. (A) Steady-state conditions: hydroxamate siderophore production was converted to C equivalents and normalized to bacterial C production as described in the text. The raw data are presented in Fig. 3. (B) Transient conditions: change in hydroxamate concentration normalized to cellular production 1 h after pulsed Fe addition. The raw data are presented in Fig. 5. The minimum estimate (○) assumed 20 fmol C $cell^{-1}$ and 10 mol C mol^{-1} hydroxamate, and the maximum estimate (●) assumed 10 fmol C $cell^{-1}$ and 22 mol C mol^{-1} hydroxamate. The solid and dashed lines in panel A represent least squares exponential regressions through the data ($p < 0.0001$); these regression lines are redrawn in panel B for reference

Dose response of siderophore production to Fe supply

An instantaneous and sustained increase in Fe concentration in the chemostat provided temporary relief of Fe limitation, judging from the rapid increase in cell density and rise in ETS activity (Figs. 6 & 7). Addition of 2 µmol Fe l^{-1} caused hydroxamate siderophore concentration to decline to 0 µmol hydroxamate l^{-1} (Fig. 6) as bacteria became Fe-sufficient and C-limited (Table 2). This result contrasted with the measurements in batch culture that showed hydroxamate siderophore was produced under Fe-replete growth (Figs. 1 & 2) and further supported the idea that C availability could modulate the response of bacteria to Fe-limiting conditions by affecting the amount of siderophore produced. At lower Fe concentrations, biomass increased (Fig. 7), but bacteria remained Fe-limited (Table 2). Little evidence for an increase in NSSR was apparent in these experiments that were supplied with much lower concentrations of Fe compared to the pulse perturbations. The increase in cell density (Fig. 7) was proportional to the concentration of Fe added as predicted from chemostat theory. Hydroxamate siderophore secretion rate increased in proportion to Fe supply rate (Fig. 8) and showed that bacteria maintained tight control over Fe availability in the medium. This response was analogous to what is observed in other species that produce Cu-binding ligands (Moffett & Brand 1996, Gordon et al. 2000) to detoxify Cu by complexation.

Comparison with Fe-fertilization experiments

The results reported here may be relevant to the ongoing discussion about the origin and identity of FeBL in Fe-fertilized, HNLC regions of the sea (Rue & Bruland 1997, Gledhill & Buck 2012). In 4 Fe-enrichment experiments conducted to date, the concentration of FeBL increased by 4- to 10-fold above pre-infusion levels roughly 1 to 2 d after Fe addition (Rue & Bruland 1997, Boye et al. 2005, Kondo et al. 2008, Adly et al. 2015). Rue & Bruland (1997) hypothesized that the ligands might be siderophores secreted by bacteria to take advantage of the Fe input. Indeed, our observation of increased NSSR immediately after pulsed Fe addition to the chemostats provides support for this idea. Although the duration of enhanced secretion was short, scaled to the bacterial metabolic rates, it occurred within 0.3 to 0.8 of a cell generation and thus was relatively similar to the duration of FeBL increase observed in the field (0.3 to 1.5 of mean cell generation time). The dose response of siderophore production to an increase in Fe concentration suggested that *P. haloplanktis* tightly regulated Fe availability in its environment and was reminiscent of the increase in FeBL observed following multiple Fe injections to HNLC waters (Rue & Bruland 1997, Boye et al. 2005, Kondo et al. 2008). A pulsed addition of Fe to the chemostats only temporarily relieved Fe deficiency in *P. haloplanktis* as it was taken up and washed out of the vessel by continuous inflow of fresh medium. Likewise, in the ocean, Fe concentration decreased soon after fertilization because of uptake, vertical and horizontal mixing, and scavenging of Fe(III) oxides by colloidal and particulate matter (Wong et al. 2006), so bacteria may quickly return to a Fe-deficient state. Indeed, measurements of Fe transport kinetics by Adly et al. (2015) showed bacteria developed signs of Fe deficiency within as little as 4 d of Fe enrichment during the SERIES experiment. A second Fe addition enhanced siderophore Fe-uptake systems and increased the expression of outer membrane siderophore receptors, suggesting that bacteria were gearing-up to use siderophore-bound Fe (Adly et al. 2015).

The simplicity of our laboratory setup may overlook some important modulators of siderophore production that would likely operate in natural systems and potentially create a positive feedback loop. For example, secretion of siderophores by some bacteria could deprive other bacteria of Fe and induce them to produce their own siderophores. Alternatively, Fe-siderophore complexes and quorum-sensing molecules (Guan et al. 2000, 2001) could positively regulate siderophore production and uptake in other strains. Such responses would increase the total amount of siderophores in the environment and create competition among the ligands for Fe binding. Heterotrophic bacteria are an incredibly diverse group known to produce a large variety of siderophore types and may have evolved many strategies to deal with natural variations in Fe concentration. Our results show that siderophore production by an Fe-limited species of γ-proteobacteria is stimulated by Fe addition. Future work should focus on representatives of other lineages and mixed populations to assess how Fe enrichment affects siderophore production and competitive outcomes under Fe-limiting conditions.

Acknowledgements. Funding was provided by grants from the Natural Sciences and Engineering Research Council of Canada and the Center for Environmental Bio-Inorganic Chemistry, Princeton University (supported by the US National Science Foundation and the US Department of Energy). We thank F. Guichard for providing useful comments on an earlier version of the manuscript.

LITERATURE CITED

Acinas SG, Anton J, Rodriguez-Valera F (1999) Diversity of free-living and attached bacteria in offshore western Mediterranean waters as depicted by analysis of genes encoding 16S rRNA. Appl Environ Microbiol 65:514–522

Adly CL, Tremblay JE, Powell RT, Armstrong E, Peers G, Price NM (2015) Response of heterotrophic bacteria in a mesoscale iron enrichment in the northeast subarctic Pacific Ocean. Limnol Oceanogr 60:136–148

Archer DE, Johnson K (2000) A model of the iron cycle in the ocean. Global Biogeochem Cycles 14:269–279

Archibald FS, DeVoe IW (1978) Iron in *Neisseria meningitidis*: minimum requirements, effects of limitation, and characteristic of uptake. J Bacteriol 136:35–48

Armstrong E, Granger J, Mann EL, Price NM (2004) Outer-membrane siderophore receptors of heterotrophic oceanic bacteria. Limnol Oceanogr 49:579–587

Arrieta JM, Weinbauer MG, Lute C, Herndl GJ (2004) Response of bacterioplankton to iron fertilization in the Southern Ocean. Limnol Oceanogr 49:799–808

Barbeau K, Rue EL, Bruland KW, Butler A (2001) Photochemical cycling of iron in the surface ocean mediated by microbial iron(III)-binding ligands. Nature 413: 409–413

Bishop JK, Davis RE, Sherman JT (2002) Robotic observations of dust storm enhancement of carbon biomass in the North Pacific. Science 298:817–821

Boye M, Nishioka J, Croot PL, Laan P, Timmermans KR, de Baar HJW (2005) Major deviations of iron complexation during 22 days of a mesoscale iron enrichment in the open Southern Ocean. Mar Chem 96:257–271

Bratbak G, Dundas I (1984) Bacterial dry-matter content and biomass estimations. Appl Environ Microbiol 48:755–757

Braun V, Hantke K, Koster W (1998) Bacterial iron transport: mechanisms, genetics, and regulation. In: Sigel A, Sigel H (eds) Metal ions in biological systems. Iron transport and storage in microorganisms, plants and animals, Vol 35. Marcel Dekker, New York, NY

Cochlan WP (2001) The heterotrophic bacterial response during a mesoscale iron enrichment experiment (IronEx II) in the eastern equatorial Pacific Ocean. Limnol Oceanogr 46:428–435

Croot PL, Bowie AR, Frew RD, Maldonado MT and others (2001) Retention of dissolved iron and Fe-II in an iron induced Southern Ocean phytoplankton bloom. Geophys Res Lett 28:3425–3428

Duce RA, Tindale NW (1991) Atmospheric transport of iron and its deposition in the ocean. Limnol Oceanogr 36: 1715–1726

Fekete FA, Spence JT, Emery T (1983) Siderophores produced by nitrogen-fixing *Azotobacter vinelandii* Op in iron-limited continuous culture. Appl Environ Microbiol 46:1297–1300

Folsom JP, Parker AE, Carlson RP (2014) Physiological and proteomic analysis of *Escherichia coli* iron-limited chemostat growth. J Bacteriol 196:2748–2761

Fourquez M, Obernosterer I, Blain S (2012) A method for the use of the radiotracer ^{55}Fe for microautoradiography and CARD-FISH of natural bacterial communities. FEMS Microbiol Lett 337:132–139

Gillam AH, Lewis AG, Andersen RJ (1981) Quantitative determination of hydroxamic acids. Anal Chem 53:841–844

Gledhill M, Buck KN (2012) The organic complexation of iron in the marine environment: a review. Front Microbiol 3:69

Gledhill M, van den Berg CMG (1994) Determination of complexation of iron(III) with natural organic complexing ligands in seawater using cathodic stripping voltammetry. Mar Chem 47:41–54

Gordon AS, Donat JR, Kango RA, Dyer BJ, Stuart LM (2000) Dissolved copper-complexing ligands in cultures of marine bacteria and estuarine water. Mar Chem 70:149–160

Granger J, Price NM (1999) The importance of siderophores in iron nutrition of heterotrophic marine bacteria. Limnol Oceanogr 44:541–555

Guan LL, Onuki H, Kamino K (2000) Bacterial growth stimulation with exogenous siderophore and synthetic *N*-acyl homoserine lactone autoinducers under iron-limited and low-nutrient conditions. Appl Environ Microbiol 66: 2797–2803

Guan LL, Kanoh K, Kamino K (2001) Effect of exogenous siderophores on iron uptake activity of marine bacteria under iron-limited conditions. Appl Environ Microbiol 67:1710–1717

Hale MS, Rivkin RB, Matthews P, Agawin NSR, Li WKW (2006) Microbial response to a mesoscale iron enrichment in the NE subarctic Pacific: heterotrophic bacterial processes. Deep-Sea Res II 53:2231–2247

Hall JA, Safi K (2001) The impact of in situ Fe fertilisation on the microbial food web in the Southern Ocean. Deep-Sea Res 48:2591–2613

Haygood MG, Holt PD, Butler A (1993) Aerobactin production by a planktonic marine *Vibrio* sp. Limnol Oceanogr 38:1091–1097

Heinrichs JH, Gatlin LE, Kunsch C, Choi GH, Hanson MS (1999) Identification and characterization of SirA, an iron-regulated protein from *Staphylococcus aureus*. J Bacteriol 181:1436–1443

Hopkinson BM, Barbeau KA (2012) Iron transporters in marine prokaryotic genomes and metagenomes. Environ Microbiol 14:114–128

Hutchins DA, Campbell BJ, Cottrell MT, Takeda S, Cary SC (2001) Response of marine bacterial community composition to iron additions in three iron-limited regimes. Limnol Oceanogr 46:1535–1545

Jacques P, Ongena M, Bernard F, Fuchs R, Budzikiewicz H, Thonart P (2003) Fluorescent *Pseudomonas* mainly produce the dihydro form of pyoverdine at low specific growth rate. Lett Appl Microbiol 36:259–262

Kondo Y, Takeda S, Nishioka J, Obata H, Furuya K, Johnson WK, Wong CS (2008) Organic iron(III) complexing ligands during an iron enrichment experiment in the western subarctic North Pacific. Geophys Res Lett 35:L12601, doi:10.1029/2008GL033354

Kudo I, Noiri Y, Cochlan WP, Suzuki K, Aramaki T, Ono T, Nojiri Y (2009) Primary productivity, bacterial productivity and nitrogen uptake in response to iron enrichment during the SEEDS II. Deep-Sea Res II 56:2755–2766

Maldonado MT, Price NM (1999) Utilization of iron bound to strong organic ligands by plankton communities in the subarctic Pacific Ocean. Deep-Sea Res I 46:2447–2473

Maldonado MT, Boyd PW, La Roche J, Strzepek R and others (2001) Iron uptake and physiological response of phytoplankton during a mesoscale Southern Ocean iron enrichment. Limnol Oceanogr 46:1802–1808

Martinez JS, Carter-Franklin JN, Mann EL, Martin JD, Haygood MG, Butler A (2003) Structure and membrane affinity of a suite of amphiphilic siderophores produced by a marine bacterium. Proc Natl Acad Sci USA 100: 3754–3759

Mawji E, Gledhill M, Milton JA, Tarran GA and others (2008) Hydroxamate siderophores: occurrence and importance in the Atlantic Ocean. Environ Sci Technol 42:8675–8680

McIntosh MA, Earhart CF (1977) Coordinate regulation by iron of the synthesis of phenolate compounds and three outer membrane proteins in *Escherichia coli.* J Bacteriol 131:331–339

Mietzner TA, Tencza SB, Adhikari P, Vaughan KG, Nowalk AJ (1998) Fe(III) periplasm-to-cytosol transporters of gram-negative pathogens. Curr Top Microbiol Immunol 225:113–135

Moffett JW, Brand LE (1996) Production of strong, extracellular Cu chelators by marine cyanobacteria in response to Cu stress. Limnol Oceanogr 41:388–395

Packard TT, Williams PJL (1981) Rates of respiratory oxygen consumption and electron transport in surface seawater from the northwest Atlantic. Oceanol Acta 4:351–358

Price NM, Harrison GI, Hering JG, Hudson RJ, Nirel PMV, Palenik B, Morel FMM (1989) Preparation and chemistry of the artificial algal culture medium Aquil. Biol Oceanogr 6:443–461

Reid RT, Butler A (1991) Investigation of the mechanism of iron acquisition by the marine bacterium *Alteromonas luteoviolaceus*: characterization of siderophore production. Limnol Oceanogr 36:1783–1792

Reid RT, Live DH, Faulkner DJ, Butler A (1993) A siderophore from a marine bacterium with an exceptional ferric ion affinity constant. Nature 366:455–458

Royer SJ, Levasseur M, Lizotte M, Arychuk M and others (2010) Microbial dimethylsulfoniopropionate (DMSP) dynamics along a natural iron gradient in the northeast subarctic Pacific. Limnol Oceanogr 55:1614–1626

Rue EL, Bruland KW (1995) Complexation of iron(III) by natural organic ligands in the Central North Pacific as determined by a new competitive ligand equilibration/absorptive cathodic stripping voltammetric method. Mar Chem 50:117–138

Rue EL, Bruland KW (1997) The role of organic complexation on ambient iron chemistry in the equatorial Pacific Ocean and the response of a mesoscale iron addition experiment. Limnol Oceanogr 42:901–910

Schattenhofer M, Fuchs BM, Amann R, Zubkov MV, Tarran GA, Pernthaler J (2009) Latitudinal distribution of prokaryotic picoplankton populations in the Atlantic Ocean. Environ Microbiol 11:2078–2093

Simon M, Azam F (1989) Protein content and protein synthesis rates of planktonic marine bacteria. Mar Ecol Prog Ser 51:201–213

Smith PK, Krohn RI, Hermanson GT, Mallia AK and others (1985) Measurement of protein using bicinchoninic acid. Anal Biochem 150:76–85

Temirov YV, Esikova TZ, Kashparov IA, Balashova TA, Vinokurov LM, Alakhov YB (2003) A catecholic siderophore produced by the thermoresistant *Bacillus licheniformis* VK21 strain. Russ J Bioorganic Chem 29:542–549

Tortell PD, Maldonado MT, Price NM (1996) The role of heterotrophic bacteria in iron-limited ocean ecosystems. Nature 383:330–332

Tortell PD, Maldonado MT, Granger J, Price NM (1999) Marine bacteria and biogeochemical cycling of iron in the oceans. FEMS Microbiol Ecol 29:1–11

Trick CG (1989) Hydroxamate-siderophore production and utilization by marine eubacteria. Curr Microbiol 18: 375–378

Velasquez I, Nunn BL, Ibisanmi E, Goodlett DR, Hunter KA, Sander SG (2011) Detection of hydroxamate siderophores in coastal and sub-Antarctic waters off the South Eastern Coast of New Zealand. Mar Chem 126:97–107

Velji MI, Albright LJ (1986) Microscopic enumeration of attached marine bacteria of seawater, marine sediment, fecal matter, and kelp blade samples following pyrophosphate and ultrasound treatments. Can J Microbiol 32:121–126

Volker C, Wolf-Gladrow DA (1999) Physical limits on iron uptake mediated by siderophores or surface reductases. Mar Chem 65:227–244

Vraspir JM, Butler A (2009) Chemistry of marine ligands and siderophores. Annu Rev Mar Sci 1:43–63

Wietz M, Gram L, Jørgensen B, Schramm A (2010) Latitudinal patterns in the abundance of major marine bacterioplankton groups. Aquat Microb Ecol 61:179–189

Witter AE, Hutchins DA, Butler A, Luther GW III (2000) Determination of conditional stability constants and kinetic constants for strong model Fe-binding ligands in seawater. Mar Chem 69:1–17

Wong CS, Johnson WK, Sutherland N, Nishioka J, Timothy DA, Robert M, Takeda S (2006) Iron speciation and dynamics during SERIES, a mesoscale iron enrichment experiment in the NE Pacific. Deep-Sea Res II 53: 2075–2094

Young RW, Carder KL, Betzer PR, Costello DK and others (1991) Atmospheric iron inputs and primary productivity: phytoplankton responses in the North Pacific. Global Biogeochem Cycles 5:119–134

Editorial responsibility: Ronald Kiene, Mobile, Alabama, USA

Submitted: October 16, 2014; Accepted: May 7, 2015
Proofs received from author(s): June 16, 2015